

Polarizabilities of rubidium (9-10)S_{1/2} and 8D_{3/2,5/2} states

 J. Walls, J. Clarke, S. Cauchi, G. Karkas, H. Chen, and W.A. van Wijngaarden^a

Physics Dept., Petrie Bldg., York University, 4700 Keele St., Toronto, Ontario, Canada M3J 1P3

Received 7 September 2000 and Received in final form 6 December 2000

Abstract. Polarizabilities of several rubidium states were determined by measuring stark shifts of transitions using an electro-optically modulated laser beam to excite an atomic beam. The voltage required for atoms excited by the laser beam in an electric field to be simultaneously in resonance as atoms excited by a frequency sideband of the laser in a field free region was measured. The scalar α_0 and tensor α_2 polarizabilities were found to be: $\alpha_0(9S_{1/2}) = 103.77 \pm 0.09$, $\alpha_0(10S_{1/2}) = 272.54 \pm 0.16$, $\alpha_0(8D_{3/2}) = 230.68 \pm 0.25$ and $\alpha_2(8D_{3/2}) = 26.55 \pm 0.10$, $\alpha_0(8D_{5/2}) = 222.68 \pm 0.14$ and $\alpha_2(8D_{5/2}) = 51.91 \pm 0.10$ MHz/(kV/cm)². The results are 100 times more accurate than previous measurements and are within 1% of those found theoretically using a Coulomb approximation calculation.

PACS. 32.60.+i Zeeman and Stark effects – 32.10.Dk Electric and magnetic moments, polarizability – 39.30.+w Spectroscopic techniques

1 Introduction

Precise measurements of polarizabilities are important to describe a number of atomic properties including charge exchange cross-sections, van der Waals constants and dielectric constants [1]. Accurate data are also needed for applications such as determining electric fields in plasmas [2]. A number of methods have been developed to measure polarizabilities and are described in several review articles [3–6]. Considerable improvements in the determination of polarizabilities have resulted from experiments that precisely measure stark shifts of transitions. The resulting polarizabilities have uncertainties that are more than one order of magnitude smaller than the uncertainties in the most accurate measurements of atomic lifetimes [7] or oscillator strengths [8]. The stark shifts of the D lines of the alkali atoms have been a favourite of experimentalists as lasers readily operate at the transition wavelengths [9–12]. In addition, alkali atoms can be simply modeled as a valence electron interacting with the Coulomb potential generated by the nucleus and inner electron core [13]. Hence, precise measurements of polarizabilities stringently test atomic theory.

Several groups have determined polarizabilities of excited alkali states. O’Sullivan and Stoicheff used a pulsed dye laser to find the polarizabilities of the (15-80)S [14] and (13-55)D [15] states of ⁸⁵Rb to an accuracy of a few percent. The group of Svanberg [16,17] used a lamp and dye laser to stepwise excite several S and D states of rubidium and cesium. An atomic beam was excited as it passed through an electric field and fluorescence was monitored as

the dye laser frequency was scanned across the resonance. The change of the laser frequency was monitored using an interferometer. Their resulting polarizabilities had uncertainties of 10%. Our group has previously determined the polarizabilities of the (10-13)S_{1/2} and (10-13)D_{3/2,5/2} states of cesium with an uncertainty of about one part in a thousand [18–20]. This paper reports polarizabilities for the (9-10)S_{1/2} and 8D_{3/2,5/2} states of rubidium that are 100 times more accurate than previously found.

The relevant terms in the Hamiltonian describing the states examined in this experiment is given by [21]

$$H = a\mathbf{L} \cdot \mathbf{S} - \left\{ \alpha_0 + \alpha_2 \frac{3L_z^2 - \mathbf{L}^2}{L(2L-1)} \right\} \frac{F^2}{2}. \quad (1)$$

The first term represents the spin orbit interaction where a is the coupling constant ($a(8D) = 12\,120$ MHz), \mathbf{L} is the orbital electronic angular momentum and \mathbf{S} is the electron spin. The second term represents the stark shift due to an external electric field F where α_0 and α_2 are the scalar and tensor polarizabilities respectively. The term containing α_2 vanishes when $L < 1$. For low electric fields, the eigenstates are approximately given by $|Jm_J\rangle$ where m_J is the azimuthal quantum number corresponding to the total electronic angular momentum J . The eigenenergies are given by:

$$E = \frac{1}{2}hKF^2 \quad (2)$$

^a e-mail: www@yorku.ca

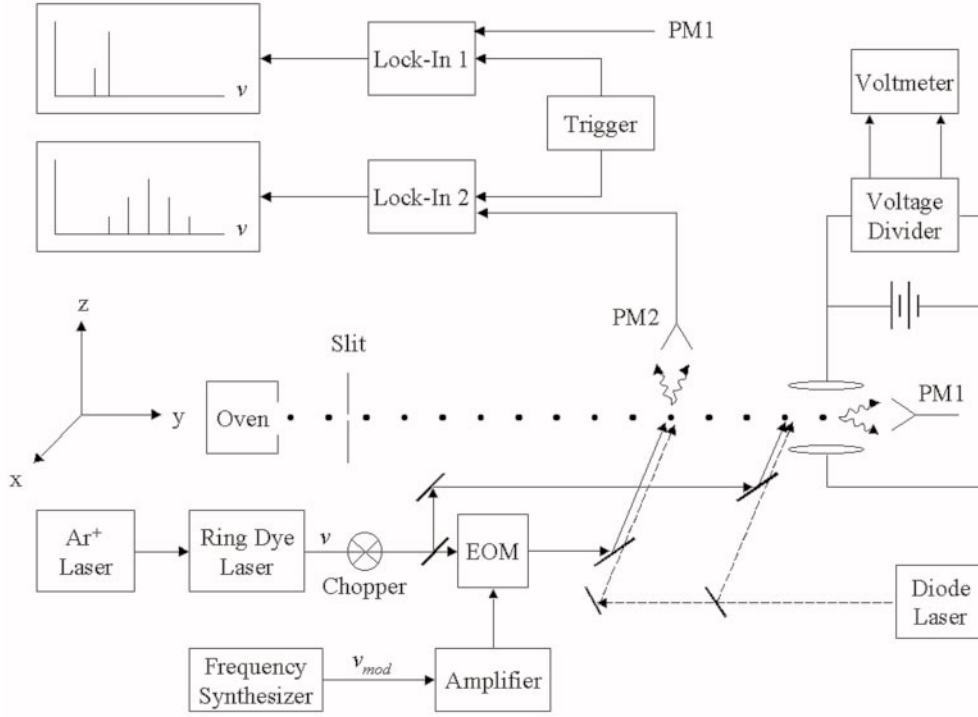


Fig. 1. Apparatus. See text for description.

where h is Planck's constant. K is called the Stark shift rate and is given by

$$K(S_{1/2}, |m_J| = 1/2) = -\alpha_0(S_{1/2}), \quad (3a)$$

$$K(D_{5/2}, |m_J| = 1/2) = -\alpha_0(D_{5/2}) + \frac{4}{5}\alpha_2(D_{5/2}) + \frac{3}{250} \frac{\alpha_2(D_{5/2})^2 F^2}{a}, \quad (3b)$$

$$K(D_{5/2}, |m_J| = 3/2) = -\alpha_0(D_{5/2}) + \frac{1}{5}\alpha_2(D_{5/2}) + \frac{9}{125} \frac{\alpha_2(D_{5/2})^2 F^2}{a}, \quad (3c)$$

$$K(D_{5/2}, |m_J| = 5/2) = -\alpha_0(D_{5/2}) - \alpha_2(D_{5/2}), \quad (3d)$$

$$K(D_{3/2}, |m_J| = 1/2) = \alpha_0(D_{3/2}) + \alpha_2(D_{3/2}) - \frac{6}{245} \frac{\alpha_2(D_{3/2})^2 F^2}{a}, \quad (3e)$$

$$K(D_{3/2}, |m_J| = 3/2) = \alpha_0(D_{3/2}) - \alpha_2(D_{3/2}) - \frac{36}{245} \frac{\alpha_2(D_{3/2})^2 F^2}{a}. \quad (3f)$$

Equation (3) does not include the Stark shift of the lower $5P_{3/2}$ state. In the data analysis the effect of $\alpha_0(5P_{3/2}) = 0.216 \text{ MHz}/(\text{kV}/\text{cm})^2$ was included while $\alpha_2(5P_{3/2}) = -0.036 \text{ MHz}/(\text{kV}/\text{cm})^2$ was negligible and therefore ignored.

2 Apparatus

The apparatus is illustrated in Figure 1. It has been described previously [19], so only a short description will be

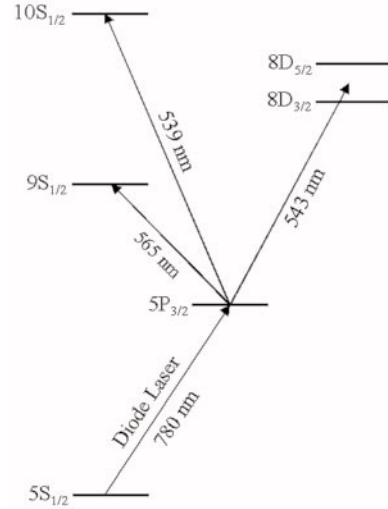


Fig. 2. Relevant states of rubidium. The diode laser excited the $5S_{1/2} \rightarrow 5P_{3/2}$ transition while a ring dye laser excited the $5P_{3/2}$ state to one of the higher states shown. The vertical energy axis is not drawn to scale.

given here. An oven was heated to about 150°C and generated a collimated rubidium atomic beam. The atomic beam traveled in a vacuum chamber that was pumped to a pressure of 1×10^{-6} torr with a diffusion pump and a liquid nitrogen trap. The rubidium atoms were excited as is illustrated in Figure 2. A diode laser generated 45 mW of light at 780 nm. It could be tuned to populate the $5P_{3/2}$ state of either ^{85}Rb or ^{87}Rb . The transitions to the $(9-10)S_{1/2}$ or $8D_{3/2,5/2}$ states were excited using a ring

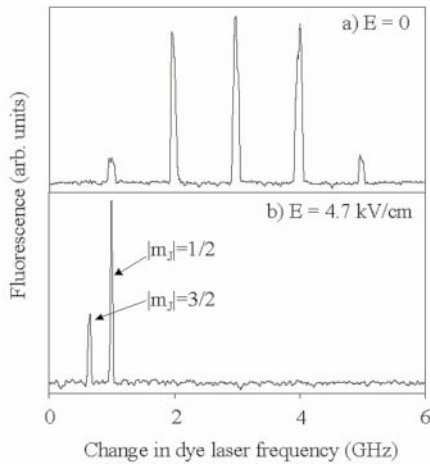


Fig. 3. Fluorescence signals. Panel (a) shows a typical signal obtained by the photomultiplier detecting fluorescence from the field free region while the signal in panel (b) resulted from detecting fluorescence emitted by atoms in the field region.

dye laser. The dye laser beam passed through an electro-optic modulator that generated frequency sidebands using a modulation frequency ν_{mod} of 1 GHz. This modulation signal was generated by a frequency synthesizer with an accuracy of one part per million.

Doppler free excitation of the atoms was achieved by having the laser beams intersect the atomic beam perpendicularly. Atoms were excited as they passed first through a field free region and subsequently through a uniform electric field. The latter was generated by applying a voltage across a pair of stainless steel plates separated by 2.5395 ± 0.0006 cm. The voltage was determined using a voltage divider having an accuracy of 0.015% and a precision voltmeter. Fluorescence, produced by the radiative decay of the atoms, was detected by two photomultipliers (PM1 and PM2) in series. The two fluorescence signals were processed by separate lock-in amplifiers whose reference was provided by a chopper that modulated the dye laser beam.

The stark shift rate was determined by measuring the electric field required for atoms excited by the dye laser beam to be simultaneously in resonance as atoms excited in the field free region by one of the frequency sidebands of the dye laser beam. A typical data scan is shown in Figure 3 for the case where the $5P_{3/2} \rightarrow 8D_{5/2}$ transition was studied. The five peaks observed in Figure 3a are separated by the 1 GHz modulation frequency which permitted the frequency scan of the dye laser to be calibrated. Only two peaks were observed in Figure 3b as the dye and diode lasers were polarized parallel to the electric field and the $|m_J| = 5/2$ levels of the $8D_{5/2}$ state were therefore not populated.

The separation of the stark shifted $|m_J| = 1/2$ peak in Figure 3b and the peak in Figure 3a generated by the -2 GHz sideband of the frequency modulated dye laser beam in the field free region was plotted *versus* the square of the electric field. Figure 4 shows data taken for the $8D_{5/2}|m_J| = 1/2$ state while Figure 5 shows data taken

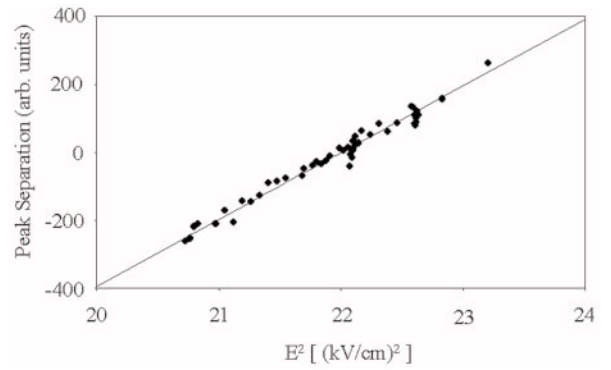


Fig. 4. Stark shift of the $8D_{5/2} |m_J| = 1/2$ level *versus* square of the electric field.

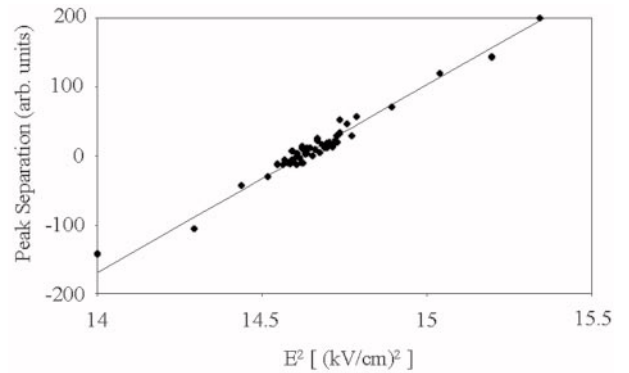


Fig. 5. Stark shift of the $10S_{1/2}$ state *versus* square of the electric field.

for the $10S_{1/2}$ state. A line $y = AF^2 + B$ was then fit to the data to find the electric field F_0 giving zero peak separation.

The stark shift rate was obtained using

$$K = \frac{2(n\nu_{\text{mod}} + \nu_{\text{off}})}{F_0^2} \quad (4)$$

where n refers to the peak generated by either the first or second order sideband of the dye laser that overlapped the stark shifted peak. ν_{off} is a small residual first order Doppler shift that arises because the laser and atomic beam intersection angles in the field free and field regions differ slightly. It was found by taking data with zero voltage applied to the plates. A typical value of ν_{off} was -9.0 ± 0.5 MHz where the negative sign indicates the atoms between the plates fluoresced just before atoms in the field free region. ν_{off} was measured several times during each data taking session to ensure that the relative alignment of the laser and atomic beams did not change.

3 Results

The scalar polarizabilities of the (9-10) $S_{1/2}$ states were found by substituting the measured stark shift rate into equation (3a). The results are listed in Tables 1 and 2. For the $8D_{3/2,5/2}$ states, the stark shift rate depends on α_0

Table 1. Check for isotope dependence of polarizabilities. Units of polarizabilities are MHz/(kV/cm)².

State	Quantity	⁸⁷ Rb	⁸⁵ Rb	Combined result
10S _{1/2}	α_0	272.50 ± 0.23	272.57 ± 0.22	272.54 ± 0.16
8D _{5/2}	α_0	222.39 ± 0.23	222.86 ± 0.18	222.68 ± 0.14
	α_2	51.80 ± 0.14	52.00 ± 0.13	51.91 ± 0.10

Table 2. Comparison of results to previous measurements and theoretical calculations. Units of polarizabilities are MHz/(kV/cm)².

State	α_0	α_2	Reference
9S _{1/2}	103.77 ± 0.09		This work
	102 ± 9		Previous expt. [17]
	103.5		Theory [23]
10S _{1/2}	272.54 ± 0.16		This work
	280 ± 25		Previous expt. [17]
	271		Theory [23]
8D _{3/2}	230.68 ± 0.25	26.55 ± 0.10	This work
	211 ± 18	27.0 ± 1.4	Previous expt. [16,17]
	232.9	26.1	Theory [23]
8D _{5/2}	222.68 ± 0.14	51.91 ± 0.10	This work
		56.9 ± 3.0	Previous expt. [17]
	224.9	52.5	Theory [23]

and α_2 . The tensor polarizability was first determined by measuring the electric field causing the $|m_J| = 1/2$ and $|m_J| = 3/2$ peaks to be separated by 1 GHz. Next, the stark shift rate for the $|m_J| = 1/2$ or $|m_J| = 3/2$ line was obtained by measuring the electric field causing this line to be stark shifted 2 GHz [22]. The scalar polarizability was then found using equation (3).

A number of experimental checks were performed. Table 1 shows that no significant difference was found when the diode laser excited either the ground state $F = 3$ hyperfine level of ⁸⁵Rb or the $F = 2$ hyperfine level of ⁸⁷Rb to the 5P_{3/2} state. The various hyperfine levels of the 5P_{3/2} state experience different stark shifts due to the tensor polarizability. In this experiment, however, $\alpha_2(5P_{3/2})$ is smaller than the uncertainties of the results listed in Table 2. The results were also found to be independent of the voltage polarity.

The error bars of the polarizabilities listed in Tables 1 and 2 take into account uncertainties associated with the electric field, frequency offset and the fitting of the data to a line as shown in Figures 4 and 5. The results agree well with previous experimental results but are about 100 times more accurate than the earlier experiment by the Svanberg group. In this experiment, a larger fluorescence signal was produced since a laser was used instead of a lamp to excite the atoms to the 5P_{3/2} state. In addition, the electric field and frequency shifts could be more precisely determined.

The results are within 1% of values computed using a Coulomb approximation calculation [23]. This theoretical

model has also been used to calculate polarizabilities of excited S and D states of cesium that are within 1% of experimental results [18–20]. A maximum discrepancy of several percent between theoretically and experimentally determined polarizabilities has only been found for the lowest P states of rubidium [23] and cesium [24]. This is not unexpected since the Coulomb approximation does not take into account the spin orbit interaction that scales as $1/r^3$ where r is the distance between the nucleus and the valence electron. Hence, it can be concluded that for nearly all states of rubidium the theoretically computed values of polarizabilities are reliable to within a percent. This is especially useful for estimating polarizabilities of states where no experimental data exists.

We would like to thank the Natural Sciences and Engineering Research Council and the Canadian Institute for Photonic Innovations for financial support. The authors gratefully acknowledge T. Scholl of the University of Western Ontario for technical advice with the dye laser. J. Walls and J. Clarke are recipients of an Ontario Graduate Scholarship in Science and Technology and a JDS Uniphase Scholarship respectively.

References

1. K.D. Bonin, M.A. Kadar-Kallen, Phys. Rev. A **47**, 944 (1993).
2. J.E. Lawler, D.A. Doughty, Adv. At. Mol. Opt. Phys. **25**, 37 (1988).

3. T.M. Miller, B. Bederson, *Adv. At. Mol. Phys.* **13**, 1 (1977).
4. T.M. Miller, B. Bederson, *Adv. At. Mol. Opt. Phys.* **25**, 37 (1988).
5. W.A. van Wijngaarden, *Adv. At. Mol. Opt. Phys.* **36**, 141 (1996).
6. W.A. van Wijngaarden, *Atom. Phys.* **16**, 305 (1999).
7. R.J. Rafac *et al.*, *Phys. Rev. A* **50**, R1976 (1994).
8. W.A. van Wijngaarden *et al.*, *Phys. Rev. Lett.* **56**, 2024 (1986).
9. C.E. Tanner, C. Wieman, *Phys. Rev. A* **38**, 162 (1988).
10. L. Windholz, M. Musso, *Phys. Rev. A* **39**, 2472 (1989).
11. L.R. Hunter *et al.*, *Opt. Commun.* **94**, 210 (1992).
12. K.E. Miller, D. Krause, L.R. Hunter, *Phys. Rev. A* **49**, 5128 (1994).
13. D.R. Bates, A. Damgaard, *Philos. Trans. Roy. Soc.* **242**, 101 (1949).
14. M.S. O'Sullivan, B.P. Stoicheff, *Phys. Rev. A* **31**, 2718 (1984).
15. M.S. O'Sullivan, B.P. Stoicheff, *Phys. Rev. A* **33**, 1640 (1986).
16. W. Hogervorst, S. Svanberg, *Phys. Scripta* **12**, 67 (1975).
17. K. Fredriksson, S. Svanberg, *Z. Phys. A* **281**, 189 (1977).
18. W.A. van Wijngaarden *et al.*, *Phys. Rev. A* **49**, R2220 (1994).
19. W.A. van Wijngaarden, J. Li, *Phys. Rev. A* **55**, 2711 (1997).
20. J. Xia, J. Clarke, J. Li, W.A. van Wijngaarden, *Phys. Rev. A* **56**, 5176 (1997).
21. A. Khadjavi, A. Lurio, W. Happer, *Phys. Rev.* **167**, 128 (1968).
22. Alternatively, one could measure the electric fields that shift the $8D_{3/2,5/2}$ $|m_J| = 1/2$ and $|m_J| = 3/2$ levels by 2 GHz and solve the two resulting equations for α_0 and α_2 . The accuracy with which α_2 is determined depends on the difference of the stark shifts separating the $|m_J| = 1/2$ and $|m_J| = 3/2$ peaks. This difference is about 300 MHz for the case of the $8D_{5/2}$ state at 4.7 kV/cm. This experiment obtains a more accurate result by measuring the electric field that generates a 1 GHz stark shift difference between the $|m_J| = 1/2$ and $|m_J| = 3/2$ peaks.
23. W.A. van Wijngaarden, *J. Quant. Spectrosc. Radiat. Transfer* **57**, 275 (1997).
24. W.A. van Wijngaarden, J. Li, *J. Quant. Spectrosc. Radiat. Transfer* **52**, 555 (1994).